Mass dependence of the transverse momenta of Au projectile fragments at 1.0*A* GeV

J. L. Chance,[1] F. P. Brady,[1] J. L. Romero,[1] S. Albergo,[2] F. Bieser,[4] Z. Caccia,[2] D. Cebra,[1] A. D. Chacon,[6] Y. Choi,[5,*] S. Costa,[2] J. B. Elliott,[5] M. L. Gilkes,[3] J. A. Hauger,[5] A. S. Hirsch,[5] E. L. Hjort,[5] A. Insolia,[2] M. Justice,[3] D. Keane,[3] J. C. Kintner,[1] V. Lindenstruth,[7] M. A. Lisa,[4] H. S. Matis,[4] M. McMahan,[4] C. McParland,[4] W. F. J. Müller,[7] D. L. Olson,[4] M. D. Partlan,[1] N. T. Porile,[5] R. Potenza,[2] G. Rai,[4] J. O. Rasmussen,[4] H. G. Ritter,[4] J. Romanski,[2] G. V. Russo,[2] H. Sann,[7] R. Scharenberg,[5] A. Scott,[3] Y. Shao,[3] B. K. Srivastava,[5] T. J. M. Symons,[4] M. Tincknell,[5] C. Tuve,[2] S. Wang,[3] P. G. Warren,[5] H. H. Wieman,[4] T. Wienold,[4] and K. Wolf[6]

(The EOS Collaboration)

[1]*University of California, Davis, California 95616*
[2]*Università di Catania & INFN-Sezione di Catania, Catania I-95129, Italy*
[3]*Kent State University, Kent, Ohio 44242*
[4]*Nuclear Science Division, Lawrence Berkeley National Laboratory, Berkeley, California 94720*
[5]*Purdue University, West Lafayette, Indiana 47907-1396*
[6]*Texas A&M University, College Station, Texas 77843*
[7]*GSI, D-64220 Darmstadt, Germany*

(Received 13 February 2001; published 18 June 2001)

The transverse momenta (p_x, p_y) of projectile fragments produced by 1.0*A* GeV ^{197}Au nuclei incident on Au and C targets have been measured. The medium and heavy fragments have p_x and p_y distributions, which are wider than predicted by models. For the Au target the widths of the distributions are significantly larger than those for C, particularly for the heavy fragments. The C distributions show a different gross structure, which may be due to the target-projectile size difference.

DOI: 10.1103/PhysRevC.64.014610 PACS number(s): 25.70.Pq, 25.75.−q, 21.65.+f

INTRODUCTION

Studies of nuclear matter and its equation of state continue to be of considerable interest. Collisions between heavy nuclei offer many possibilities for systematic studies of this nature. However, these are not straightforward due to the transient and complex nature of such collisions and the fact that only properties of final products can be measured. Comprehensive sets of data and calculations are necessary in order to interpret the collisions and extract information concerning the properties of nuclear matter.

Systematic studies of the collective flow of particles, induced by nuclear collisions, were first carried out in the global analyses of collision events captured by the nearly 4π plastic ball/wall [1,2] and streamer chamber [3] detector systems. Collective flow was observed in a range of rapidities populated by participant nucleons and their composites, while ''bounce-off'' nucleons and light composites were found near projectile rapidities. These two effects were predicted in early hydrodynamic-like calculations of the compression effects in the collisions [4].

A comprehensive set of nuclear collision measurements over a wide range of projectile and target nuclei and for a range of energies, (250–1970)*A* MeV, have been carried out at the Bevalac by the EOS Collaboration [5,13]. The analysis of flow and its energy dependence for the Au+Au system [6] and for the Ni+Cu and Ni+Au systems [7] have been published. Agreement with Boltzmann-Uehling-Uhlenback (BUU) calculations is better for predictions based on an equation-of-state (EOS) with stiff (larger *K*) compressibility, or with a smaller *K* when substantial momentum dependence interaction strength is included [7]. At this point, the BUU and relativistic quantum molecular dynamics (RQMD) models do not predict the motion of the ''spectator'' nucleons as collective fragments. However, one expects that some compressional energy will be transmitted to these spectator pieces of nuclear matter. In fact, in earlier experiments at the Bevalac [8,9], a transverse momentum component of heavy fragments produced in the fragmentation of a range of nuclei (Ar to Au), was identified. These first measurements for heavier projectiles, ^{93}Nb, ^{139}La, and ^{197}Au, showed that the transverse momentum distributions, particularly those of the heavier fragments, are considerably broader than predicted by the models of Goldhaber [10] (Fermi gas) and Lepore and Riddell (LR) [11] (shell model). On the other hand, the pioneering fragmentation measurements of Greiner *et al.* [12] using light projectiles, found momentum component distribution widths for ^{16}O and ^{12}C projectile fragments, which clustered between the Goldhaber [10] and LR [11] predictions.

Here, we present measurements of the transverse (p_x and p_y) momentum components of projectile fragments from 1.0*A* GeV ^{197}Au on Au and C targets.

EXPERIMENT AND RESULTS

The measurements were taken using the EOS time projection chamber (TPC) [13] [in the 1.3T heavy ion spectrometer system (HISS) field] and the multiple sampling ionization

*Present address: Sungkyunkwan University, Suwon, Korea.

chamber (MUSIC) [14]. References [5,15] have a description and sketch of the EOS detection system. The TPC, via multiple sampling of dE/dx, provided good particle identification and separation for *p*, *d*, *t*, and He particles and for light ions with rigidities extending at least up to $\simeq 1.5$ GeV/c. MUSIC [14] has three TPC's which measure successively *x*, *y*, and *x* coordinates, each 16 times, for up to $48 dE/dx$ samples. This produces excellent charge ($\sigma_Z \approx 0.1$ to $0.2|e|$) and position resolution [14] ($\sigma_x \approx 100$ to 300 μ, except for very light fragments). The poorest σ_x is found with the heavy beams, probably due to the large number of δ rays, etc. The MUSIC momentum resolution is dominated by multiple Coulomb scattering (MCS). Both the angle uncertainty, $\delta\theta$(MCS), and θ, the fragment bend angle in the magnetic field, are nearly proportional to Z/p(p=momentum), so the momentum resolution is approximately constant. For the Au beam, $\delta\theta_b$(MCS)≈ 3.0 and 2.3 mrad for the Au and C target, respectively; for the fragments, the expected scaling $\delta\theta_F$(MCS)$=\delta\theta_b$(MCS)*(A_F/197) is assumed. The projectile fragments have $p \approx p_0 A_F$ where p_0 is the momentum per nucleon of the projectile, and A_F the mass number of the fragment. Thus the range of rigidities, proportional to that of A_F/Z_F, varies by about 20%.

The basic event trigger was set at minimum bias; off-line, events with the largest fragment charge having $Z_F \gtrsim 10$ were selected, as discussed below.

The fragment momentum component p_y is the easiest to determine and has the smallest uncertainty. The direction *y* is perpendicular to the bending plane, so one only needs to measure the vertical deflection angle θ_y. This amounts to measuring the *y* coordinates of the track in MUSIC: The middle TPC measures the *y* position 16 times. This determines both an average *y* and a vector in the *y* plane. The incoming projectile momentum, $p_P = p_0 A_P$, has its direction determined by two detectors (called Plutos) separated by 2.2 m. Each Pluto consists of a thin plastic scintillator viewed by four phototubes symmetrically arranged [15]. An *x*-*y* grid of scintillating fibers is used to provide an absolute position calibration. For Au beams, position resolution is near $\sigma_x \approx \sigma_y \approx 0.65$ mm, and $\delta\theta_b$(MCS)≈ 0.5 mrad. The target spot can also be determined by the TPC tracking of particles back to a vertex.

Analyses of the measurements of magnetic rigidity (p_F/Z_F) and energy loss produce as shown in Fig. 1, a plot of p_F/p_0 (assumed to be A_F) vs (detected) charge Z_F for fragments from 1.0*A* GeV ^{197}Au beam incident on an Au target. The squares trace the valley of nuclide stability. [The intensity falloff at large $Z_F(A_F)$ is due to the trigger condition.] Charges can be separated, but not A_F values. However, the A_F resolution, $\sigma(A_F) \simeq 3\%$, is good enough to test (see later) the fragmentation models. It can be seen in Fig. 1 that the detected fragments have a fragment mass centroid locus which, for $Z_F > 40$, lies on the proton rich side of the stability line. This phenomenon is well known from target fragmentation studies; see, for example, Sümmerer *et al.* [16]. The solid line in Fig. 1 is a prediction for the most probable fragment based on their empirical parametrization [16]. For the case of 1.0*A* GeV Au on a C target, see Fig. 11 of

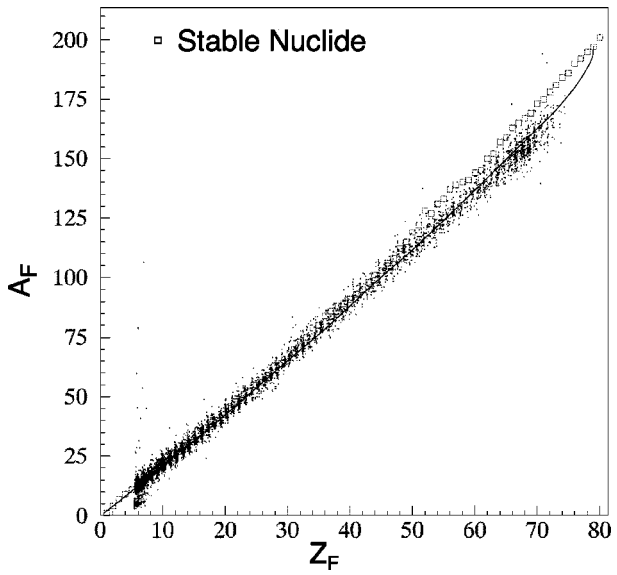

FIG. 1. Mass fragment A_F, derived from the rigidity, vs charge of detected fragments for 1.0*A* GeV Au+Au. The squares trace the valley of nuclide stability. The full line is the prediction from the parametrization of Sümmerer *et al.* [16].

Hauger *et al.* [15], who also found good agreement with the parametrization of Ref. [16]. One expects that the abrasion fragment, or prefragment, as defined in the abrasion-ablation (AA) model [17], would (immediately after collision) have, on average, a Z/A ratio close to that of the projectile. However, following excess neutron emission from the highly excited prefragment, the neutron-to-proton ratio is considerably reduced. The expected dispersion in *Z* and *A* (abrasion) has been estimated [18] using a model based on the assumption of a clean-cut, sudden interaction AA model and on the assumption of zero-point vibrations of neutrons against protons in the giant dipole resonance. This produces abrasion-stage dispersions in Z/A of $\approx 2\%$. The ablation stage will produce further dispersion and probably accounts for the larger measured A_F dispersions seen in Fig. 1.

The basic *AA* model only describes noncentral collisions and assumes that one large abrasion fragment (prefragment) results. The small branching to fission is ignored, as is multifragmentation, which dominates central collisions. Here we focus on events where at least one large fragment with $A_F \gtrsim 20$ is produced, and study the transverse momentum components of the largest Z_F. The production of heavy, proton-rich fragments from Au projectiles has been measured earlier [19] and shows that neutron emission dominates the ablation stage. This is in accord with the AA model [20] (and statistical models) wherein low-energy neutron emission is favored since the corresponding final nuclear state has higher excitation and higher (nuclear) state density. The Coulomb barrier inhibits low-energy proton, alpha, etc., emission to the higher-excitation, higher-state density regions. This AA model [20] assumes an excitation energy, which is a broad distribution with a mean near 13 MeV per ''hole'' (per nucleon removed) in the abrasion stage.

Figure 2 shows the corrected values of the standard de-

viations, $\sigma(p_x)$ and $\sigma(p_y)$, for the p_x and p_y momentum distributions vs $\langle A_F \rangle$, where $\langle A_F \rangle$ is the mean value of A_F for each Z_F determined from data such as that used for Fig. 1. The corrections include the effects of multiple scattering and beam angular dispersion. The measured beam angular width was used to calibrate the corrections to the fragment momentum widths. The uncertainties in the $\sigma(p_x)$ data shown in Fig. 2 reflect the uncertainties in these corrections and are calculated (or estimated) to be 27 (15)%, 18 (12)%, and 9 (6.5)% for $A_F = 150$, 100, and 50 for the Au (C) targets, respectively. $\sigma(p_y)$ uncertainties are 15%–30% smaller than those for $\sigma(p_x)$ with differences increasing with $\langle A_F \rangle$. The p_x and p_y distributions should be the same, but p_x is in the bending plane and its determination is more uncertain.

ANALYSES AND MODEL COMPARISONS

The Fermi gas, independent particle model used by Goldhaber [10] assumes that the only correlation among the momenta of the nucleons in the projectile and fragment is that imposed by momentum conservation. In the projectile frame this model predicts that the momentum distribution of the projectile fragments will be described by

$$\sigma^2(p_x) = \sigma^2(p_y) = \sigma^2(p_z) = \sigma_0^2 A_F (A_P - A_F)/(A_P - 1); \tag{1}$$

$\sigma_0^2 = P_F^2/5$, where P_F is the Fermi momentum in the projectile nucleus. ($P_F = 265$ MeV/c for nuclei near Au [21].) The model of LR [11] assumes shell-model wave functions with harmonic-oscillator Gaussian factors. The prediction of these two models are shown in Fig. 2(a) along with the experimental values of $\sigma(p_x)$ and $\sigma(p_y)$ for 1.0A GeV Au+Au. Here, at this point, we use the mean mass of the detected fragment $\langle A_F \rangle$ for the data and for the predictions of the two models, e.g., $A_F = \langle A_F \rangle$ in Eq. (1). It can be seen that the experimental widths are larger than the model predictions, which are based solely on the projectile nucleon internal momenta. When first observed this for heavy fragments [9], this extra width was attributed to the collision dynamics and called p_T(bounce). A simple model [9] was used to calculate the p_T brought in by nucleons scattered into the spectator from the participant (overlap) region.

Figure 2(b) shows similar comparisons for the Au+C data. Note that, vs $\langle A_F \rangle$, the structure in the data is different from that in Fig. 2(a). As one goes to $\langle A_F \rangle$ values above $\simeq 90$, the momentum widths decrease and are considerably smaller than the Au+Au values [Fig. 2(a)]. For smaller $\langle A_F \rangle$ the Au and C target values are comparable. This suggests Coulomb effects and in addition, a smaller impulse from the smaller C target or rather its optical or mean-field potential in more peripheral collisions. For $\langle A_F \rangle \lesssim 90$, one can imagine the C nucleus sometimes trying to tunnel through the Au nucleus and imparting $\langle p_T \rangle$ to the fragments.

The Goldhaber model predicts a $\sigma_0, \sigma_0(G)$, which is nearly a factor of 2 larger than σ_0(LR): For Au projectiles $\sigma_0(G)$ is near 118 and σ_0(LR) near 59.4 MeV/c. The larger momentum component widths predicted by Goldhaber, arise from the fact that nucleons, abraded from the projectile [leaving A_F(abr)], have an uncorrelated Fermi gas motion, while in the LR case, pair momenta are anticorrelated and reduce the fragment momentum produced by the abrasion. Bertsch [22] has shown for the case of ^{40}Ar fragmentation, how momentum anticorrelations suppress p_z fluctuations of the fragments.

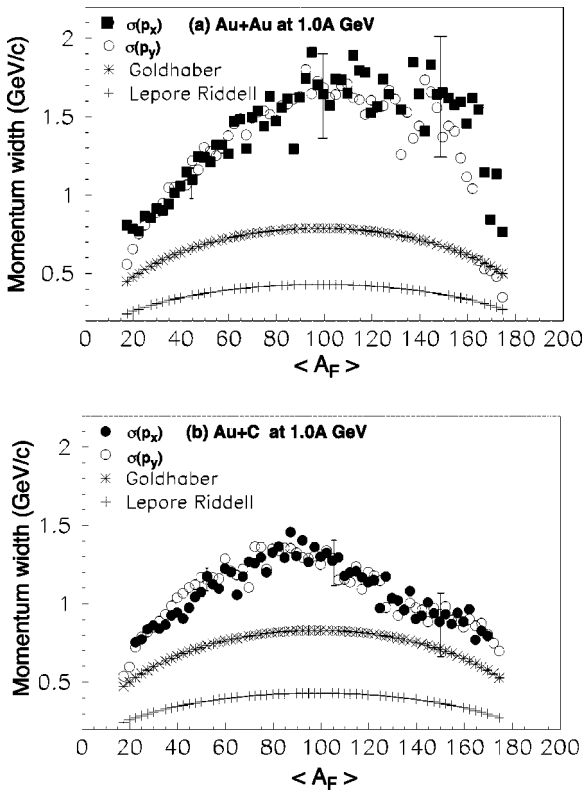

FIG. 2. Experimental (a) Au+Au and (b) Au+C transverse component momentum widths $\sigma(p_x)$ and $\sigma(p_y)$ vs $\langle A_F \rangle$. Error bars are shown for representative σ_x values (see the text). Also shown are predictions of the Goldhaber and the Lepore-Riddell models.

Figure 3 shows values of σ_0(expt) (expt=experimental) determined from the $\sigma(p_x)$ and $\sigma(p_y)$ data in Fig. 2. The σ_0(expt) values are, in general, larger than the model predictions of Goldhaber, and even larger than those of Lepore and Riddell. Subsequently, there have been theoretical calculations [23], which show that Pauli blocking reduces the Goldhaber values by nearly 50%. These calculations support the notion that, for projectile fragments, the LR values, based as they are on shell model-type wave functions, are more realistic in describing projectile-frame momentum distributions due to the internal nucleon momenta in the projectile. (The x and y values of σ and σ_0 should be the same.)

Strictly speaking, to compare to the predictions of the abrasion models, one should use the abrasion fragment masses, rather than detected fragment masses as were used in Figs. 2 and 3. This would shift the data to larger $\langle A_F \rangle$ but would not change the conclusions concerning the model comparisons above. Also, in connection with the model comparisons, the effects of a statistically nonisotropic particle (mainly neutron) emission have not been corrected for. We estimate [9] these corrections to be small except at very

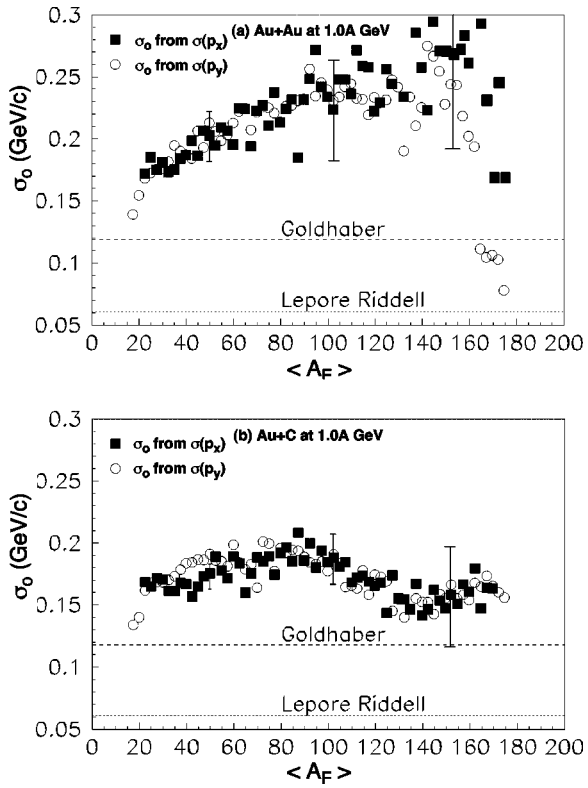

FIG. 3. Values of (a) Au+Au and (b) Au+C σ_o derived from values in Fig. 2 vs $\langle A_F \rangle$, with representative error bars (see the text).

small $\sigma(p_x)$, $\sigma(p_y)$ values; i.e., where, in these data, A_F approaches A_P.

While the σ_0(expt) values derived here from $\sigma(p_x)$ and $\sigma(p_y)$ are considerably larger than the model values, it is interesting to note that the longitudinal (p_z) component widths as measured at GSI for 1.0*A* GeV Au+Au [24], are found to be narrower than the Goldhaber predictions. The corresponding σ_0(expt) values appear to lie in between Goldhaber and LR, but closer to the LR predictions, and in good agreement with the experimental systematics of Morrissey *et al.* [25] Thus, as expected, the collision dynamics, e.g., the collective effects as modeled by a hydrodynamical model, affect the transverse momentum more than the longitudinal.

The above discussion indicates that the ''intrinsic'' contributions from internal nucleon momenta to the production of the experimental transverse momentum component distribution widths, are relatively small. With all effects included, the corresponding σ_0 values are probably near 50 MeV/c. We might call these intrinsic: σ_0(intr). The σ_0(expt) values (Fig. 3) range largely between $\simeq$125 and 250 MeV/c, or considerably larger than σ_0(intr). Originally, we hypothesized that the additional p_T we first saw in the 1.2*A* GeV ^{139}La+C fragmentation [9], had a Coulomb component, p_T(Coul), and a component due to the participant nucleons transferring energy and momentum to the ''spectator'' fragment. With reasonable assumptions for the nucleon p_T values from *NN* (*N*=nucleon) collisions and for nucleon mean-free-paths in nuclear matter, the large p_T values of the fragments could be understood [9].

In terms of a macroscopic (hydrodynamic) model, one can speak of the transfer of compressional energy to the prefragment and hence to the detected fragment. The contribution p_T(Coul) can be estimated for grazing collisions [26] as p_T(Coul)=1432 and 156 MeV/c or p_x(Coul)=p_y(Coul) =1014 and 110 MeV/c for Au+Au and Au+C [27], respectively. One concludes that Coulomb effects are important, and in Fig. 2 one sees, particularly for the heavy fragments up to $\langle A_F \rangle$=165, that the sigma values are progressively larger as one goes from the data for the C target to that of Au targets. Kahn *et al.* [27] present an ''optical-model momentum transfer'' formalism, which they use to successfully describe the 1.2*A* GeV ^{139}La+C fragment transverse momentum component (p_y) distributions [9]. They also fit the 980*A* MeV Au+Ag $\sigma_x(\sigma_y)$ data [28]. The latter data [9] and the Au+CR-39 (plastic detector) data [28] at 980*A* MeV are, within limited statistics, consistent with our data.

Goldhaber [10] has suggested that if the projectile nucleus receives a collision impulse Q in some direction, the mean-squared momentum transfer in that direction would increase from σ^2 due to nucleon momenta (intrinsic) to

$$\sigma'^2 = \sigma^2 + Q^2 (A_F/A_P)^2 \tag{2}$$

for the fragment of mass A_F, where the transverse components of σ^2 (due to projectile nucleon momenta) are given by Eq. (1) with the above estimates that $\sigma_0 \simeq 50$ MeV/c. In this case (model) [10] the momentum distribution of the heaviest fragments is most sensitive to the collision impulse Q. Comparing the data for Au and C targets, one concludes that Q has a large A_T as well as (see Ref. [8]) A_P dependence. The structure of Q is not within the scope of this paper, e.g., in a collective model it will (as noted above) contain nuclear matter compressional, as well as Coulomb, effects.

SUMMARY

The heavy fragments from 1.0*A* GeV ^{197}Au on Au and C targets show enhanced transverse momentum components when compared to the predictions of models based on nucleon momentum distributions in nuclei. The momentum distributions tend to be larger for the Au target, particularly for the $A_F \gtrsim 100$ fragments. For the C target the $\sigma(p_x)$ and $\sigma(p_y)$ structure may be due to the target-projectile size difference.

ACKNOWLEDGMENTS

The authors are pleased to acknowledge helpful communications and AA model data from M. de Jong, A. Junghans, and K.-H. Schmidt of GSI, and the support of the U.S. National Science Foundation, the U.S. Department of Energy, Associated Western Universities, the National Aeronautics and Space Administration, and the German Federal Ministry of Research and Development; and the assistance of the Bevalac Operations Support Groups.

[1] H. Å. Gustafsson, H. H. Gutbrod, G. Kolb, H. Löhner, B. Ludewigt, A. M. Poskanzer, T. Renner, H. Riedesel, H.-G. Ritter, A. Warwick, F. Weik, and H. Weiman, Phys. Rev. Lett. **52**, 1590 (1984).

[2] H. H. Gutbrod, K. H. Kampert, B. Kolb, A. M. Poskanzer, H.-G. Ritter, R. Schicker, and H. R. Schmidt, Phys. Rev. C **42**, 640 (1990).

[3] R. E. Renfordt, D. Schall, R. Bock, R. Brockmann, J. W. Harris, A. Sandoval, R. Stock, H. Ströbele, D. Bangert, W. Rauch, G. Odyniec, H. G. Pugh, and L. S. Schroeder, Phys. Rev. Lett. **53**, 763 (1984).

[4] W. Scheid, H. Müller, and W. Greiner, Phys. Rev. Lett. **32**, 741 (1974); J. Hofmann, W. Scheid, and W. Greiner, Nuovo Cimento A **33**, 343 (1976); J. Hofmann, H. Stöcker, Un. Heinz, W. Scheid, and W. Greiner, Phys. Rev. Lett. **36**, 88 (1976).

[5] H. Wieman *et al.*, Nucl. Phys. **A525**, 617c (1991); S. Costa for the EOS Collaboration, Proceedings of the 23rd International Winter Meeting on Nuclear Physics, Bormio, Italy, 1994.

[6] M. Partlan *et al.*, the EOS Collaboration, Phys. Rev. Lett. **75**, 2100 (1995).

[7] J. L. Chance *et al.*, the EOS Collaboration, Phys. Rev. Lett. **78**, 2535 (1997).

[8] F. P. Brady *et al.*, Phys. Rev. C **50**, R525 (1994).

[9] F. P. Brady, W. B. Christie, J. L. Romero, C. E. Tull, B. McEachern, M. L. Webb, J. C. Young, H. J. Crawford, D. E. Greiner, P. J. Lindstrom, and H. Sann, Phys. Rev. Lett. **60**, 1699 (1988); W. B. Christie, J. L. Romero, F. P. Brady, C. E. Tull, G. P. Grim, B. McEachern, J. C. Young, H. J. Crawford, D. E. Greiner, P. J. Lindstrom, H. Sann, and U. Lynen, Phys. Rev. C **48**, 2973 (1993).

[10] A. S. Goldhaber, Phys. Lett. **53B**, 306 (1974); H. Feshbach and K. Huang, *ibid.* **47B**, 300 (1973).

[11] J. V. Lepore and R. J. Riddell, Jr., Report No. LBL-3086, 1976 (unpublished), give $\sigma_0^2(\mathrm{LR}) = m_p(45P^{-4/3} - 25P^{-5/3})(P - 1)/2(\mathrm{MeV}/c)^2$, where m_p is the proton mass in MeV/c^2 and P is the projectile nucleus mass number.

[12] D. E. Greiner, P. J. Lindstrom, H. H. Heckman, B. Cork, and F. S. Bieser, Phys. Rev. Lett. **35**, 153 (1975). The published momentum distributions are for p_z, but the authors note that p_x and p_y distributions are similar to within 10%.

[13] G. Rai *et al.*, IEEE Trans. Nucl. Sci. **37**, 56 (1990).

[14] G. Bauer *et al.*, Nucl. Instrum. Methods Phys. Res. A **386**, 249 (1997). A mark I MUSIC and principles is described in W. C. Christie *et al.*, *ibid.* **255**, 466 (1987).

[15] J. A. Hauger *et al.*, the EOS Collaboration, Phys. Rev. C **57**, 764 (1998).

[16] K. Sümmerer, W. Brüchle, D. J. Morrissey, M. Schädel, B. Szweryn, and Yang Weitan, Phys. Rev. C **42**, 2546 (1990).

[17] Y. Eisenberg, Phys. Rev. **96**, 1378 (1954); J. D. Bowman, W. J. Swiatecki, and C. F. Tsang, Report No. LBL-2908, 1973 (unpublished); J. Gosset *et al.*, Phys. Rev. C **16**, 629 (1977).

[18] D. J. Morrissey, W. R. Marsh, R. J. Otto, W. Loveland, and G. T. Seaborg, Phys. Rev. C **18**, 1267 (1978).

[19] W. R. Binns, J. R. Cummings, T. L. Garrard, M. H. Israel, M. P. Kertzmann, J. Klarmann, E. C. Stone, and C. J. Waddington, Phys. Rev. C **39**, 1785 (1989).

[20] J.-J. Gaimard and K.-H. Schmidt, Nucl. Phys. **A531**, 709 (1991).

[21] E. J. Moniz *et al.*, Phys. Rev. Lett. **26**, 445 (1971).

[22] G. N. Bertsch, Phys. Rev. Lett. **46**, 472 (1981).

[23] M. J. Murphy, Phys. Lett. **135B**, 25 (1984).

[24] W. J. F. Müller *et al.* (private communication).

[25] D. J. Morrissey, Phys. Rev. C **39**, 460 (1989).

[26] J. D. Jackson, *Classical Electrodynamics*, 2nd ed. (Wiley, New York, 1975), p. 619, Eq. (13.1).

[27] F. Kahn, G. S. Khandelwal, L. W. Townsend, and J. W. Wilson, Phys. Rev. C **43**, 1372 (1991).

[28] J. Dreute, W. Heinrich, G. Rusch, and B. Wiegel, Phys. Rev. C **47**, 415 (1993).